

See discussions, stats, and author profiles for this publication at: <https://www.researchgate.net/publication/236633740>

Relationship between cloud droplet effective radius, liquid water content, and droplet concentration for warm clouds in Brazil embedded in biomass smoke

Article · March 1999

DOI: 10.1029/1998JD200119

CITATIONS

62

READS

161

4 authors, including:



[Jeffrey S. Reid](#)

United States Naval Research Laboratory

230 PUBLICATIONS 8,137 CITATIONS

SEE PROFILE

Relationships between cloud droplet effective radius, liquid water content, and droplet concentration for warm clouds in Brazil embedded in biomass smoke

Jeffrey S. Reid,¹ Peter V. Hobbs, Arthur L. Rangno, and Dean A. Hegg

Department of Atmospheric Sciences, University of Washington, Seattle

Abstract. During the Smoke, Clouds, and Radiation-Brazil (SCAR-B) project, the microphysical properties of over 1000 warm, nonprecipitating, clouds were measured from the University of Washington research aircraft. The clouds were partially embedded in the continental-scale, smoky haze that envelops much of Brazil during the biomass-burning season. For the entire data set, the most universal parameterization for the effective cloud droplet radius (r_{eff}) is as a function of the ratio of cloud liquid water content (LWC) to droplet concentration (essentially the volume mean radius, r_v); this agrees with previous studies under less polluted conditions. Comparisons of SCAR-B data with data from the east coast of the United States and clean oceanic areas show that the r_{eff} - r_v relationship is similar in all three cases, suggesting that even the extreme case of clouds impacted by large biomass fires can be treated similarly to more typical clouds. Beyond a certain ambient concentration of accumulation-mode particles (~ 3000 – 4000 cm^{-3}), cloud drop number concentrations for cumulus clouds in Brazil were almost constant, so that further increases in the ambient particle concentration did not change r_{eff} and r_{eff} correlates well with LWC alone. For example, a cumulus cloud, which capped a particularly large smoke plume with total particle concentrations $>150,000$ cm^{-3} , had the same r_{eff} -LWC relationship as other clouds in the region where the ambient particle concentrations were ~ 3000 cm^{-3} . In this study the values of r_{eff} for cumulus clouds in Brazil affected by smoke were between 3 and 8 μm , compared to 9 to 14 μm inferred from satellite measurements of cloud reflectivity at 3.7 μm by Kaufman and Fraser [1997].

1. Introduction

During the dry season (July through October) biomass burning produces major increases in the atmospheric fine particle loading in the Amazon Basin and cerrado regions of Brazil [Artaxo *et al.*, 1994]. Smoke from thousands of individual fires undergoes photochemical and cloud processing to form a regional haze that covers millions of square kilometers. This haze can be over 3 km thick and have fine particle mass concentrations >150 $\mu\text{g m}^{-3}$ and optical depths that are frequently greater than 2 [Reid *et al.*, 1998; Ross *et al.*, 1998]. Recent studies of the optical properties of biomass-burning aerosols have shown that their globally averaged direct radiative forcing is less than previously assumed [Hobbs *et al.*, 1997]. Only a few studies have investigated the effects of smoke aerosol on cloud properties and therefore their indirect radiative forcing [Kaufman and Nakajima, 1993; Kaufman and Fraser, 1997]. Although smoke particles have relatively low hygroscopicities [Kotchenruther and Hobbs, 1998], they can be relatively effective cloud condensation nuclei [Warner and Twomey, 1967; Hobbs and Radke, 1969; also Q. Ji *et al.*, manuscript in

preparation, 1998]. Therefore, since there is frequently cloud cover over the Amazon Basin in the dry season and these clouds are often partially embedded in regional smoky hazes, there is significant potential for the smoke from biomass burning to alter cloud microphysical properties and hence cloud albedo.

This paper is concerned with the relationship between the cloud droplet effective radius, cloud liquid water content, and droplet concentration for the extreme case of clouds affected by aerosol from biomass burning in Brazil. The effective radius, r_{eff} , is defined as

$$r_{eff} = \int_0^\infty r^3 n(r) dr / \int_0^\infty r^2 n(r) dr \quad (1)$$

where, $n(r)$ is the number concentration of drops of radius r . The parameter r_{eff} is of considerable interest because it determines many important radiative properties of a cloud, including cloud albedo [Hansen and Travis, 1974].

For a monodispersed distribution of droplets of radius r (μm) present in number concentration N (cm^{-3}), the liquid water content (LWC in g m^{-3}) is given by

$$10^6 \text{ LWC} = \frac{4}{3} \pi r^3 N \rho_L \quad (2)$$

where ρ_L is the density of liquid water ($=1$ g cm^{-3}). Therefore

$$r = 100 \left(\frac{3 \text{ LWC}}{4 \pi N} \right)^{1/3} \quad (3)$$

¹Now at Propagation Division, Space and Naval Warfare System Center, San Diego, California.

This expression applies also to a polydispersed droplet distribution if r is replaced by the droplet radius of average volume (r_v). If the droplet size distribution is such that $r_v \approx r_{eff}$ (as it is for a monodispersed population of droplets) then

$$r_{eff} \approx 100 \left(\frac{3 \text{LWC}}{4\pi N} \right)^{1/3} \quad (4)$$

Hence if the LWC is known (from measurements or from a numerical cloud model), r_{eff} can be estimated from (4) for various assumed values of N .

Blyth and Latham [1991] and Bower *et al.* [1994] analyzed cumulus clouds in both marine and continental regions. The results of this study suggest that (4) can be used in cases where the LWC approximates the adiabatic value (i.e., the droplets are unaffected by dry air entrainment). Further, (4) can be used for the parameterization of small cumulus and layer clouds in global climate models (if they compute cloud LWC) by assuming $N = 600 \text{ cm}^{-3}$ for small continental cumulus or stratocumulus clouds. For deep convective continental clouds, Bower *et al.* suggested that r_{eff} be considered to have a constant value of $10 \text{ }\mu\text{m}$. Martin *et al.* [1994] also found (4) adequately represents stratiform clouds if N is replaced by kN , where k is an empirical factor ($k=0.80\pm0.07$ and 0.67 ± 0.07 for marine and continental air masses, respectively). Martin *et al.* [1994] suggested that rather than assuming $r_{eff} = r_v$, it is more reasonable to assume that r_{eff} and r_v are proportional. Gerber [1996] and Liu and Hallett [1997] showed that for an assumed size distribution of cloud droplets, r_{eff} is proportional to $(\text{LWC}/N)^{1/3}$.

In this paper we present the results of extensive measurements of r_{eff} , LWC, and N for extremely polluted cumulus clouds (i.e., those with very high values of N) that form in widespread regional palls of smoke from biomass burning in Brazil. Since particles from biomass burning are good cloud condensation nuclei, the value of N for cumulus clouds in Brazil can reach values as high as 1400 cm^{-3} . We will see to what extent (4) can be fitted to these extremely polluted clouds, and we will test various parameterizations for r_{eff} in terms of LWC and N .

2. SCAR-B Field Project

In August and September 1995, the University of Washington (UW) Convair C-131A research aircraft participated in the Smoke, Clouds, and Radiation-Brazil (SCAR-B) field project [Kaufman *et al.*, 1998]. One of the main goals of SCAR-B was to obtain measurements of the physical, chemical, and radiative properties of the palls of smoke that cover millions of square kilometers of the Amazon Basin and the cerrado regions of Brazil during the burning season, and to investigate the effects of the smoke on aerosol radiative forcing. Over 1000 cumuliform boundary layer clouds, with bases embedded in regional hazes dominated by smoke, and with various heights and at various stages in their development, were sampled from the C-131A aircraft. Droplet number concentrations in these clouds ranged from 100 to $1,400 \text{ cm}^{-3}$, LWC from 0.05 to 2 g m^{-3} , and r_{eff} from 3 to $9 \text{ }\mu\text{m}$.

Flight operations were conducted from four bases: Brasilia (the capital of Brazil, 14°S , 48°W), Cuiabá (in the state of Mato Grosso, 16°S , 56°W), Porto Velho (Rondonia, 9°S ,

64°W), and Marabá (Pará, 5°S , 49°W). Brasilia and Cuiabá are in the cerrado region (savanna/grassland), and Porto Velho and Marabá in the western and eastern portions of the Amazon Basin, respectively. Since the aerosols around Brasilia had a strong urban component, clouds in this region are not discussed here.

3. Instrumentation

The instrumentation on the C-131A aircraft and the data collected in SCAR-B are described by P. V. Hobbs (unpublished report, 1996, available on the World Wide Web at <http://cargsun2.atmos.washington.edu>). Therefore only a brief description is given here.

Smoke particle concentrations were generally measured with a TSI 3760 condensation nucleus (CN) counter. For the few cases where CN concentrations were greater than $40,000 \text{ cm}^{-3}$, CN concentrations were measured with a modified GE CNC-2 condensation nucleus counter. It should be noted that smoke particle diameters were almost always greater than $0.1 \text{ }\mu\text{m}$, with count median diameters ranging from 0.12 to $0.2 \text{ }\mu\text{m}$ [Reid *et al.*, 1998], and nucleation modes were very rarely detected (since fine-mode smoke particle concentrations were high, ranging from 20 to $200 \text{ }\mu\text{g m}^{-3}$, homogenous nucleation of aerosol was thermodynamically unfavorable). Therefore in this paper CN refers to accumulation-mode particles only.

Cloud liquid water contents were measured with a Gerber particle volume monitor (PVM)-100A microphysics probe [Gerber *et al.*, 1994]. Cloud droplet size distributions were measured with a Particle Measuring System, Inc. (PMS) forward scattering spectrometer probe (FSSP)-100 for droplets with radii between 1 and $25 \text{ }\mu\text{m}$, and with a PMS one-dimensional (1-D) optical array probe (OAP)-200X for droplets with radii between 10 and $150 \text{ }\mu\text{m}$. Because the FSSP-100 has a tendency to undercount the number of drops at high LWC, the number concentration of droplets measured by the FSSP-100 in each bin was multiplied by a constant so that the LWC derived from the FSSP-100 matched that measured by the PVM-100A. This resulted in an a shift in N derived from the FSSP-100 by $<20\%$. FSSP-100 data were also corrected using the activity correction of Baumgardner [1983]. After applying these corrections, the total sizing uncertainty for the FSSP-100 is estimated to be about $\pm 28\%$ [Baumgardner *et al.*, 1990]. From comparisons with the other cloud LWC probes on the UW C-131A (Johnson Williams and the King probes), we estimate that the LWCs given in this paper are within $\pm 20\%$ of their true values.

The effective radius of the cloud droplets was calculated from their size distributions measured by the FSSP-100 (radius between 1 and $25 \text{ }\mu\text{m}$) and the OAP probe (radius $>25 \text{ }\mu\text{m}$)

$$r_{eff} = \left[\sum_{i=1}^M r_i^3 n_i \left/ \sum_{i=1}^M r_i^2 n_i \right. \right]^{-1} \quad (5)$$

where M is the total number of size channels used, r_i the mean droplet radius, and n_i the number concentration of droplets in channel i . Each data point used in this analysis was derived from 1 s averages when the aircraft was flying in cloud.

The PVM-100A also yields the effective radius of the cloud droplet spectrum. Results from the PVM agreed with those derived from the FSSP-100 to within $\pm 0.5 \text{ }\mu\text{m}$, and they

reproduce all of the qualitative features presented in this paper. Because we used the same FSSP-100, and the same data corrections for this instrument, in all of the field studies for which data are shown in this paper, we present only FSSP-100 data.

4. Conditions and Clouds Studied

Airborne measurements of regional hazes dominated by smoke from biomass burning were obtained in the vicinity of Cuiabá (August 24 to September 1), Porto Velho (September 5–13), and Marabá (September 16–18). At all three locations the mixed layer generally extended through a height of 1 km, and the convective boundary layer (CBL) extended to the trade inversion (~3 km). Also, at all of these locations, aerosol fine particle mass loadings in the mixed layer varied from ~30 to 150 $\mu\text{g m}^{-3}$, and CN concentrations from ~2000 to 10,000 cm^{-3} . A source apportionment study suggests that over 70% of the aerosol mass was from biomass burning [Reid *et al.*, 1998]. Roughly 50% of the smoke particles were active as cloud condensation nuclei (CCN) at 0.5% supersaturation (Q. Ji *et al.*, manuscript in preparation, 1998).

During SCAR-B the C-131A aircraft flew a total of about 250 km in cumulus humilis, cumulus mediocris, and cumulus congestus clouds. The clouds included in the present study were warm (i.e., contained no ice) and at the time of sampling produced no detectable precipitation. Roughly 35% of the clouds were penetrated in the lowest third of their depth, 45% in the middle third, and 20% in the uppermost third.

Eighty-two clouds were sampled in Cuiabá, 472 clouds in Porto Velho, and 459 in Marabá. In Cuiabá, cumulus humilis or altocumulus located near the top of the trade inversion were generally present. Liquid water contents in Cuiabá rarely rose above 0.5 g m^{-3} , and cloud widths varied from 90 m to 1 km. In Porto Velho, midafternoon skies tended to be covered ~30–60% by cumulus mediocris and cumulus congestus, with cloud bases between 700 and 1000 m (i.e., well within the 3 km deep haze layer). Sampled clouds had widths ranging from 120 m to 4 km. Cloud tops usually reached no more than 4 km and LWC < 1.5 g m^{-3} . However, by midday, 10 km deep cumulonimbus were observed on occasions. In Marabá there was a further increase in convective activity, with more than 50% sky coverage by large cumulus mediocris and cumulus congestus (sampled cloud widths varied from 200 m to 4 km).

Twelve "fumulus" clouds, which formed above large fires, were also sampled. Most of these clouds had high interstitial particle concentrations (20,000 to 80,000 cm^{-3}), moderate droplet concentrations (~600 cm^{-3}), but extremely low LWC (< 0.05 g m^{-3}). However, on one occasion a very large fire (which produced CN > 150,000 cm^{-3}) spawned a large cumulus congestus cloud.

5. Results

5.1. Cumulus Clouds

A plot of r_{eff} versus LWC for all of the cumulus clouds sampled is shown in Figure 1. Despite the large number of data points from many different types of cumulus clouds (>2500 one second data points), and the wide range of CN concentrations at cloud base (from 1000 to hundreds of thousands cm^{-3}), there is a clear functional relationship between r_{eff} and LWC. For LWC < 0.5 g m^{-3} (indicative of

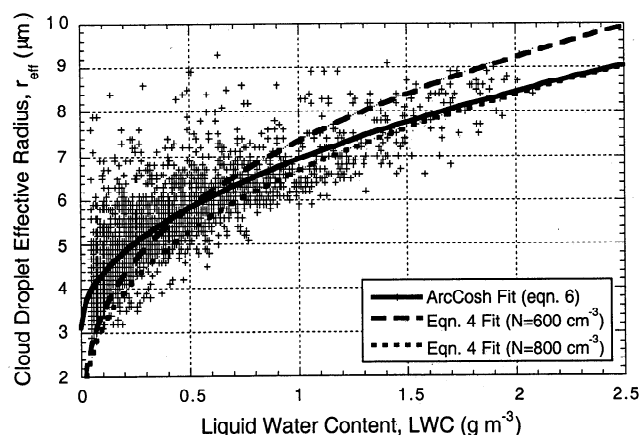


Figure 1. Cloud droplet effective radius (r_{eff}) versus liquid water content (LWC) for all of the cumulus clouds sampled from the UW C-131A aircraft in SCAR-B.

small clouds and the dying stages of larger clouds), r_{eff} was generally between 4 and 6 μm . For LWC > 0.5 g m^{-3} , r_{eff} and LWC are almost linearly related (with $r_{\text{eff}} \approx 8.5 \mu\text{m}$ for a LWC of 2 g m^{-3}).

Many parameterizations were tried to achieve the best curve fit for all of the data shown in Figure 1, including linear, power law, logarithmic, and hyperbolic functions. The best fit was given by

$$r_{\text{eff}} = (2.9 \pm 0.1) + (2.7 \pm 0.4) \text{arccosh}[1 + (1.3 \pm 0.5) \text{LWC}]$$

$$(r^2 = 0.68) \quad (6)$$

Relationship (6) is plotted in Figure 1 as the solid line. With an r^2 value of 0.68 (i.e., almost 70% of the variance accounted for), and with the standard deviation of data points across the line of less than 0.7 μm , this function provides a good predictor of r_{eff} for known values of LWC for the warm cumulus clouds.

If we restrict the data to cumulus clouds over Porto Velho, the corresponding best fit relationship is

$$r_{\text{eff}} = (2.9 \pm 0.1) + (2.8 \pm 0.4) \text{arccosh}[1 + (1.4 \pm 0.5) \text{LWC}]$$

$$(r^2 = 0.83) \quad (7)$$

and for cumulus clouds over Marabá

$$r_{\text{eff}} = (3.1 \pm 0.1) + (2.7 \pm 1.0) \text{arccosh}[1 + (1.0 \pm 0.9) \text{LWC}]$$

$$(r^2 = 0.67) \quad (8)$$

The various numerical coefficients in (7) and (8) are well within the standard error of the corresponding coefficients in (6). Regressions for the data stratified by sampling altitude, or stage of cloud development, produce no significant changes in the values of the numerical coefficients. Therefore, because the data shown in Figure 1 derive from several locations in Brazil and represent a wide range of aerosol concentrations, cumulus cloud types (with different updraft velocities and entrainments), and cloud sample heights, (6) should be valid for warm, nonprecipitating cumulus clouds embedded in continental-scale smoke plumes in Brazil.

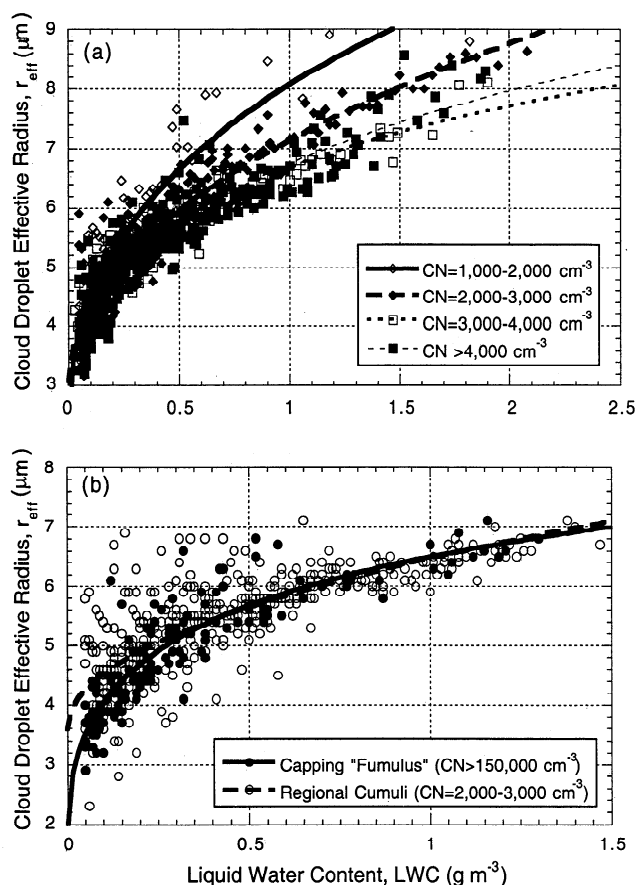


Figure 2. (a) Same as Figure 1 but for cumulus clouds sampled with accumulation-mode CN concentrations from 1000–2000 cm^{-3} (open diamonds), 2000–3000 cm^{-3} (solid diamonds), 3000–4000 (open squares), and >4000 cm^{-3} (solid squares). To reduce the density of the data points, averages were taken of triple data points having the closest liquid water content (LWC). Arccosh curve fits to the data are shown. (b) Same as Figure 1 but for a cumulus cloud that capped a large individual smoke plume (solid circles) compared to data from other cumulus clouds in the region (open circles). All 1 s data points are shown.

There were some slight differences in r_{eff} for the dirtier and the cleaner clouds sampled in SCAR-B. In Figure 2a, r_{eff} versus LWC is plotted for cases with accumulation-mode CN concentrations in the range 1000–2000 cm^{-3} , 2000–3000 cm^{-3} , 3000–4000 cm^{-3} and >4000 cm^{-3} . It can be seen that while there is a shift in r_{eff} (for a given LWC) when the CN concentration changes from 1000–2000 cm^{-3} to 2000–3000 cm^{-3} , and to 3000–4000 cm^{-3} , there is no significant change in r_{eff} when CN concentrations increase above about 4000 cm^{-3} .

For clouds of similar size, and with similar CN concentrations as the "clean" cases in SCAR-B (CN = 1000–2000 cm^{-3}), *Leitch et al.* [1992] and *Novakov et al.* [1994] found a positive correlation between non-sea-salt sulfate and cloud droplet number concentration. Hence there was likely an anticorrelation between non-sea-salt sulfate and r_{eff} for their data, similar to the anticorrelation between CN (in the range 1000–4000 cm^{-3}) and r_{eff} shown in Figure 2a.

The invariance of r_{eff} to increases in the concentration of accumulation-mode particles at high CN concentrations is

further supported by the following case. During one midmorning flight in the vicinity of Marabá (UW flight 1712), the C-131A aircraft flew a vertical profile in a region with 70% coverage of cumulus mediocris and cumulus congestus clouds. The ambient particle concentrations in the vicinity of the clouds varied from 2500 to 3500 cm^{-3} , and the adiabatic LWC was 1.4 g m^{-3} . One-second average values of r_{eff} versus LWC from a pass through the middle of these clouds are shown by the open circles in Figure 2b. Shortly after these clouds were sampled, a very large forest fire developed. This fire was so large that at an altitude of 3 km the smoke plume had an estimated updraft velocity of 15 m s^{-1} , CN concentrations of over 150,000 cm^{-3} , and a particle mass concentration of 2,500 $\mu\text{g m}^{-3}$. A large capping cumulus congestus (which later developed into a cumulonimbus) formed quickly over this fire. The cumulus congestus had a cloud base only slightly lower than the other clouds in the region. The C-131A aircraft made one pass through this cloud at a level similar to that used to characterize the other clouds in Figure 2b. The data from this pass are shown by the solid circles in Figure 2b. Examination of the two data sets in Figure 2b shows the r_{eff} versus LWC relationship is essentially the same for both cases, even though the ambient CN concentration was $\sim 3000 \text{ cm}^{-3}$ in one case and $\sim 150,000 \text{ cm}^{-3}$ in the other.

Bower et al. [1994] suggested that for deep convective continental clouds r_{eff} can be approximated as a constant of 10 μm . It can be seen from Figure 1 that this is not the case for the convective clouds we studied in Brazil. Shown in Figure 1 is (4) with $N=600 \text{ cm}^{-3}$ (recommended by *Bower et al.* [1994] for continental clouds), and the best fit of (4) to the data which is for $N=800 \text{ cm}^{-3}$. Because of the shape of the $r_{\text{eff}}-(\text{LWC})^{1/3}$ power law, (4) gives values for r_{eff} that are too low at low LWC and too high at high LWC. Furthermore, the regression coefficients (r^2) provided by (4) with $N=600$ or 800 cm^{-3} are only about 0.25 and 0.48, respectively.

One problem with (4) is that it forces r_{eff} to be zero when $\text{LWC}=0$. The FSSP-100 and OAP probes are designed to measure "typical" clouds with mass mean droplet radii above the nominal size cutoffs of these instruments ($r \sim 1 \mu\text{m}$). In even mildly polluted environments, soluble compounds in cloud drops can produce many haze particles with sizes below $r \sim 1 \mu\text{m}$. In cases such as SCAR-B, where CN concentrations were high, appreciable LWC may exist in droplets below 1 μm . At such low LWC values, the difference between "cloud" and "haze" is purely semantic. Hence as the apparent cloud LWC approaches zero, the apparent r_{eff} can converge to a nonzero value, and a nonzero converging parameterization may be necessary.

5.2. Stratocumulus Clouds

Although both (4) and (6) provide simple parameterizations of r_{eff} for cumulus clouds embedded in smoky hazes, they did not hold as well for stratocumulus clouds in Brazil. One such stratocumulus cloud layer was measured on flight 1707 in Porto Velho (Figure 3). On this flight the C-131A aircraft spent 6 minutes in cloud ($\sim 30 \text{ km}$). Data in Figure 3 are segregated into two classifications: cloud parcels with accumulation-mode CN concentrations <10,000 cm^{-3} and >10,000 cm^{-3} . For CN concentrations <10,000 cm^{-3}

$$r_{\text{eff}} = (4.4 \pm 0.7) + (1.2 \pm 0.9) \text{arccosh}[1 + (6 \pm 18) \text{LWC}]$$

$$(r^2 = 0.23)$$

$$(9)$$

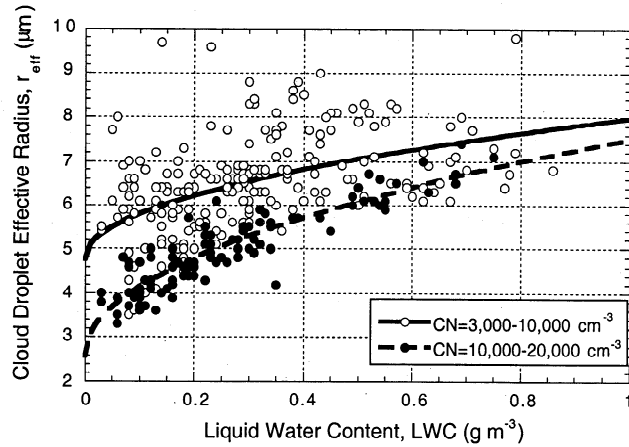


Figure 3. As for Figure 2a but for stratocumulus clouds. The data are segregated into cases where the accumulation-mode CN concentrations were between 3000 and 10,000 cm^{-3} , and between 10,000 and 20,000 cm^{-3} .

and for CN concentrations $>10,000 \text{ cm}^{-3}$

$$r_{\text{eff}} = (2.4 \pm 0.4) + (2.7 \pm 0.4) \text{arccosh}[1 + (2.1 \pm 0.3) \text{LWC}] \quad (r^2 = 0.77) \quad (10)$$

It can be seen from the r^2 value for (9) that for CN concentrations $<10,000 \text{ cm}^{-3}$, the r_{eff} versus LWC relationship is weak. However, for particle concentrations $>10,000 \text{ cm}^{-3}$, the variance in r_{eff} versus LWC for the stratocumulus clouds is much less (see equation (10)). This suggests that when maximum supersaturations are low (as in stratiform clouds), particle concentrations and chemistry significantly affect the r_{eff} versus LWC relationship, even when CN concentrations are relatively high. This type of behavior is predicted by expressions that relate cloud droplet concentration, CCN, and updraft velocity [Twomey, 1959].

Since the data presented in Figure 3 are from just one flight, they cannot be used to draw definitive conclusions. Droplet concentrations in the clouds might well be positively correlated with updraft velocity. Hence one cannot establish whether the effect of CN concentration on the LWC- r_{eff} relationship is causal. However, it is clear that it is not as easy to derive reliable r_{eff} values from LWC values for stratocumulus clouds as it is for convective clouds.

5.3. Ratio of LWC to N

The results from this study support the hypothesis of Blyth and Latham [1991], Martin et al. [1994], and Liu and Hallett [1997] that a generalized "1/3" power law exists between r_{eff} and LWC/N . Assuming the following size distribution for the droplets (Weibull distribution)

$$n^*(r) = N_0 r^{b-1} \exp(-\lambda r^b) \quad (11)$$

Liu and Hallett (see also Gerber [1996]) showed that

$$r_{\text{eff}} = \alpha(b)(\text{LWC}/N)^{1/3} \quad (12)$$

where

$$\alpha(b) = \frac{3\Gamma(3/b)}{2\Gamma(2/b)} \left(\frac{b}{4\pi\rho_w\Gamma(3/b)} \right)^{1/3} \quad (13)$$

and Γ is the gamma function,

$$\Gamma(t) = \int_0^\infty z^{t-1} \exp(-z) dz \quad (14)$$

The expressions (11) and (12) can also be expressed as

$$r_{\text{eff}} = \alpha_1(b)r_v \quad (15)$$

where

$$\alpha_1(b) = \frac{3^{2/3}\Gamma^{2/3}(3/b)}{2\Gamma(2/b)} b^{1/3} \quad (16)$$

Relationship (16) is a more general form of (4). Martin et al. [1994] used a similar empirical formulation of (4) to (16). Here, $\alpha_1(b)$ is equal to $k^{-1/3}$, where k is the droplet number concentration coefficient proposed by Martin et al. Liu and Hallett suggested that the value of α_1 or the factor k used by Martin et al. can be adjusted to account for the effect of physical processes such as entrainment and mixing in different cloud types. They also suggested that rather than plotting r_{eff} versus LWC, one should plot r_{eff} versus LWC/N , and hence determine values of b for different cloud types and environments.

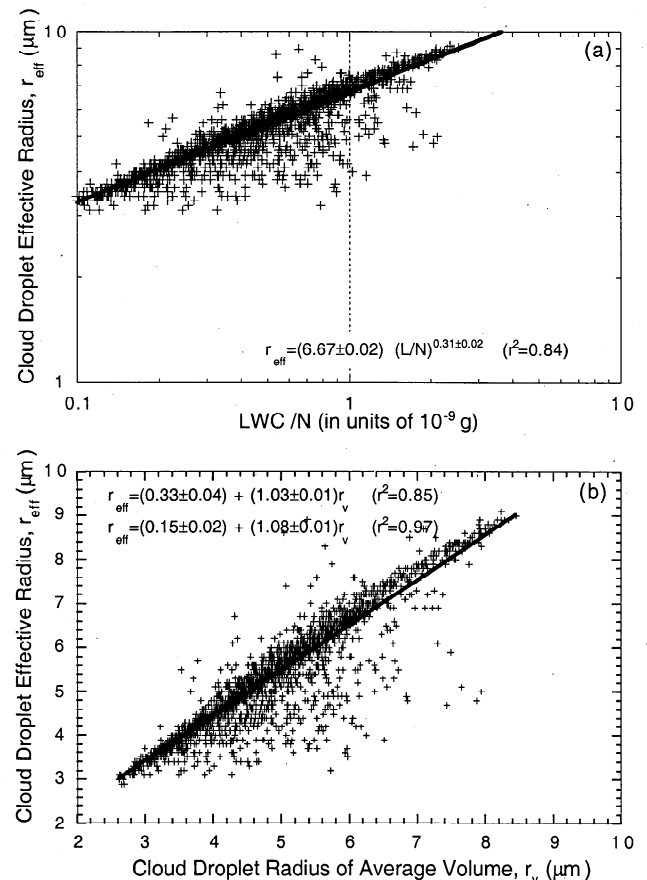


Figure 4. (a) Cloud droplet effective radius (r_{eff}) versus LWC/N for the cumulus clouds. (b) Cloud droplet effective radius (r_{eff}) versus the cloud droplet radius of average volume (r_v).

Figure 4a shows the regression of r_{eff} on LWC/N for the same cumulus cloud samples plotted in Figure 1. The results show that as suggested by Gerber [1996] and Liu and Hallett [1997], a "1/3" power law exists between r_{eff} and LWC/N. The regression relation is

$$r_{eff} = (6.67 \pm 0.02) (LWC/N)^{0.31 \pm 0.02} \quad (r^2 = 0.84) \quad (17)$$

Using the same data, we can determine the value of α_1 by plotting r_{eff} versus r_v (Figure 4b). A linear regression of the data in this figure shows that the average value of α_1 for the cumulus clouds in the SCAR-B data set is 1.03 ± 0.01 (i.e., $r_{eff} \approx r_v$). However, examination of the data in Figure 4 shows that for the over 2500 data points presented, ~75 "outliers" have a significant effect on the regression. These data points were not associated with any particular CN concentration or cloud type. If these 75 outliers are removed from the regression (i.e., a 3% trim), we obtain a value for α_1 of 1.08 ± 0.01 . Hence, at worst, r_{eff} differs from r_v by no more than 10% for Brazilian cumulus clouds affected by smoke.

A similar analysis was performed on the stratocumulus data (Figure 5), with the data segregated into CN concentrations less than and greater than $10,000 \text{ cm}^{-3}$. In contrast to the r_{eff} versus LWC relationship (Figure 3), the r_{eff} to LWC/N and the r_{eff} versus r_v relationships for the stratocumulus clouds are more structured. As for the cumulus clouds, an approximate "1/3" power law holds between r_{eff} and LWC/N for the stratocumulus clouds,

$$r_{eff} = (7.50 \pm 0.05) (LWC/N)^{0.33 \pm 0.01} \quad (r^2 = 0.79) \quad (18)$$

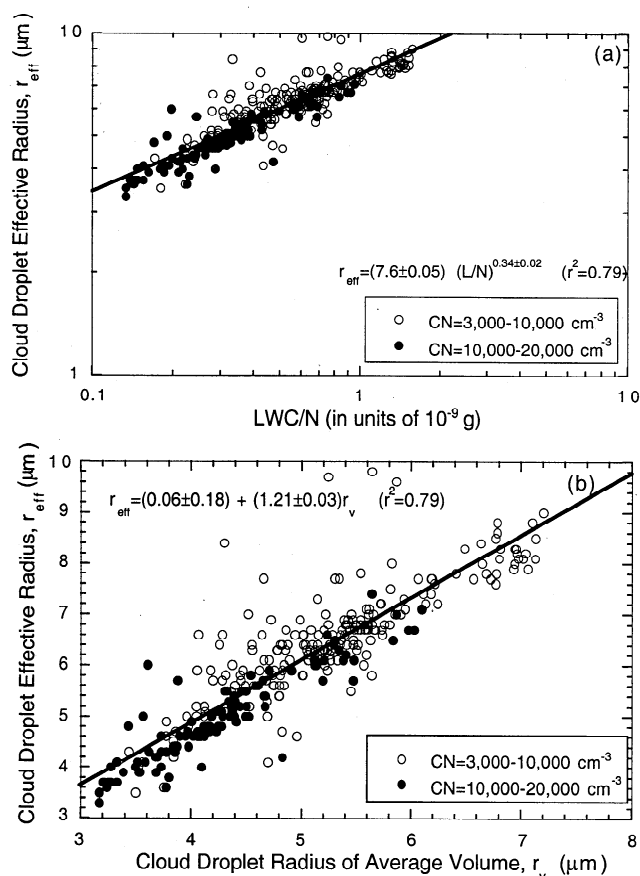


Figure 5. As for Figure 4 but for stratocumulus clouds.

Comparing this r^2 value with those in (9) and (10), we see that LWC/N provides a substantially better predictor of r_{eff} than does LWC alone. For the stratocumulus clouds, $r_{eff} = (1.21 \pm 0.03) r_v$ (compared to $r_{eff} = (1.08 \pm 0.01) r_v$ for the cumulus clouds). Based on studies of stratocumulus clouds embedded in continental air masses Martin *et al.* [1994] found $r_{eff} = (1.14 \pm 0.05) r_v$. Allowing for uncertainties in the measurements, these data are consistent with those presented here. Also, our results for polluted stratocumulus clouds in SCAR-B are not statistically different from stratocumulus clouds in other continental air masses.

Martin *et al.* [1994], Gerber [1994], and Liu and Hallett [1997] discussed the effects of particle size parameters, entrainment, and mixing on the r_{eff} versus r_v relationship for cumulus and stratocumulus clouds. Interestingly, unlike the r_{eff} versus LWC relationship (Figure 3), CN concentrations did not appear to affect the r_{eff} to r_v relationship. Even though data with $r_{eff} < 5 \mu\text{m}$ are predominately for $CN > 10,000 \text{ cm}^{-3}$, the data from the two ranges of CN concentration fall on same regression line in Figure 5. This supports the hypothesis that once a critical CCN concentration is reached, further increases in particle concentrations do not significantly affect the droplet size distribution.

6. Comparison With Data From Other Locations

The relationship between r_{eff} and LWC for cumulus clouds embedded in biomass smoke presented in this paper is similar to that for data collected by our group in other strongly polluted environments, but significantly different from the relationship for much cleaner environments. Figure 6 compares cumulus cloud data from Brazil (SCAR-B), the northeastern Atlantic Ocean (Atlantic Stratocumulus Transition Experiment (ASTEX) [Garrett and Hobbs, 1995; Gerber *et al.*, 1996]), and the east coast of the United States (Tropospheric Aerosol Radiative Forcing Experiment (TARFOX) [Russell *et al.*, 1999]).

During ASTEX, stratocumulus, altocumulus, cumulus, and cumulus congestus clouds were sampled from the UW C-131A aircraft. However, in this paper the only data from ASTEX that are shown are for warm, nonprecipitating cumulus and cumulus congestus of similar sizes and structures to those we studied in Brazil. Total particle (CN) concentrations in these clouds varied from less than 100 to 400 cm^{-3} (~10 to 20% of the CN values in Brazil), and LWC varied from 0.01 to 1.6 g m^{-3} (compared to 0.01 to 2.0 g m^{-3} in Brazil). For the ASTEX data the best parameterization between r_{eff} and LWC was

$$r_{eff} = (5.2 \pm 0.86) + (1.6 \pm 0.2) \text{arccosh}[1 + (21 \pm 22) \text{LWC}] \quad (r^2 = 0.36) \quad (19)$$

Comparing (6) and (19), two marked differences are apparent. First, as expected, the r_{eff} values for SCAR-B are 3 to $6 \mu\text{m}$ smaller than for the ASTEX data, which were obtained in much cleaner conditions. Second, the variance in the ASTEX data about (19) is twice that of the SCAR-B data about (6), despite the fact that the ASTEX data include variations in cloud types and sampling heights similar to those of the SCAR-B data. Furthermore, since the SCAR-B data were collected over an area of several thousand square kilometers, they might be expected to show much greater variance than the ASTEX data. A possible reason for the much stabler

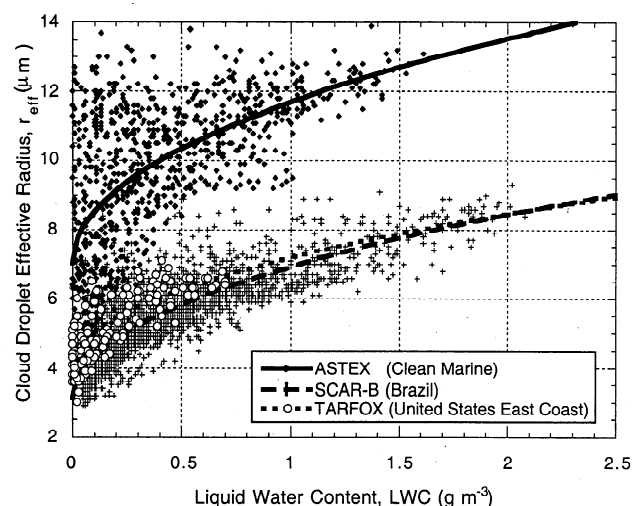


Figure 6. Cloud droplet effective radius (r_{eff}) versus liquid water content (LWC) for cumulus clouds in clean marine air over the northeastern Atlantic Ocean (diamonds, Atlantic Stratocumulus Transition Experiment (ASTEX)), in urban-industrial air off on the U.S. east coast (circles, Tropospheric Radiative Forcing Experiment (TARFOX)), and in air masses dominated by smoke from biomass burning (pluses, Brazil).

relationship in Brazil is that the numbers of activated cloud droplets (N) were likely limited by the amount of available condensate, rather than the copious CCNs that were available.

In TARFOX the C-131A aircraft flew a series of vertical profiles off the U.S. Atlantic seaboard. Air masses were sampled that had high loadings of anthropogenic pollutants (fine particle mass and CN concentrations as high as $100 \mu\text{g m}^{-3}$ and 3000 cm^{-3} , respectively). About 50 cumulus clouds, mostly cumulus humilis, were sampled. A comparison of these data with those from SCAR-B (Figure 6) shows an interesting feature. Even though the chemical compositions of the particles in these two studies were quite different (carbonaceous species and soluble sulfates in TARFOX, and mostly insoluble organic particles from biomass burning in SCAR-B), the r_{eff} versus LWC relationship is nearly the same for both data sets. The best curve fit for the TARFOX data is

$$r_{eff} = (3.5 \pm 0.4) + (1.4 \pm 0.8) \text{arccosh}[1 + (6 \pm 11) \text{LWC}] \quad (r^2 = 0.61) \quad (20)$$

Because almost all of the TARFOX data points lie in a region with $\text{LWC} < 0.5 \text{ g m}^{-3}$, where the arccosh function is not sensitive, there is a larger uncertainty in the value of the third regression variable in (20) (namely, 6 ± 11). However, the regression line is similar to that found for the SCAR-B data. The value of r_{eff} for the TARFOX data set is about $1 \mu\text{m}$ larger than for the SCAR-B data for $\text{LWC} < 0.4 \text{ g m}^{-3}$. This slight difference in r_{eff} is most likely due to the fact that the cumulus clouds in TARFOX had smaller vertical developments, lower vertical velocities and supersaturations, and therefore fewer activated particles than in SCAR-B.

It is interesting to compare the relationship between r_{eff} and LWC/N for the SCAR-B, ASTEX, and TARFOX data sets. Droplet r_{eff} versus LWC/N and droplet r_{eff} versus r_v for the ASTEX and TARFOX cases are shown in Figures 7a and 7b,

respectively. As for SCAR-B, Figure 7a shows that the "1/3" power law holds for the clouds in ASTEX and TARFOX. Further, for the TARFOX case, $r_{eff} = 1.09 r_v$ (Figure 7b). Thus the value for α_1 (1.09) for TARFOX is very close to the value of 1.08 for SCAR-B (1.03 if all the 75 outliers are included). For the clean marine cumulus clouds studies in ASTEX, $r_{eff} = 1.18 r_v$.

7. Implications for Modeling Indirect Forcing by Smoke Aerosols

Kaufman and Fraser [1997] used advanced very high resolution radiometer (AVHRR) data to estimate the effects of smoke particles on r_{eff} and cloud reflectivity for warm continental clouds, such as those we studied in Brazil. For such clouds embedded in smoky hazes over Brazil, they derived values for r_{eff} of $9\text{--}13 \mu\text{m}$, and cloud albedos from 0.30 to 0.45 ($\lambda = 580\text{--}680 \text{ nm}$). Kaufman and Fraser found that at low latitudes ($< 10^\circ$) the optical depth of the smoke was positively correlated with cloud reflectivity and anticorrelated with r_{eff} . This implies that variations in smoke concentration affect r_{eff} . In contrast, our in situ measurements suggest that most cumulus clouds embedded in smoke in Brazil have r_{eff} values of $5\text{--}8 \mu\text{m}$, and r_{eff} is insensitive to particle concentration. How can these different results be reconciled? We discuss below four possibilities for the differences in the derived values of r_{eff} .

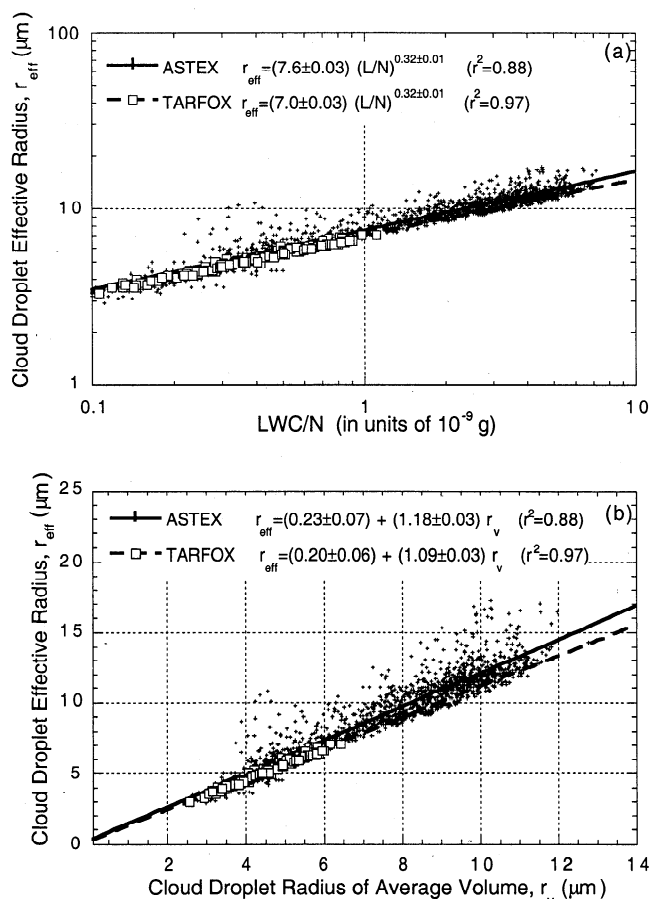


Figure 7. As for Figure 4, but for data collected over the northeast Atlantic Ocean (ASTEX) and on the U.S. east coast (TARFOX).

1) Kaufman and Fraser noted that the impact of smoke particle concentration on clouds is correlated with precipitable water vapor (PWV). They hypothesized that in areas of higher PWV more droplets are activated in clouds, possibly due to higher updraft velocities in larger clouds. In SCAR-B we observed, as expected, that larger clouds with higher updraft velocities at lower latitudes were present at higher values of PWV. However, we did not find a difference in the r_{eff} -LWC relationship at different latitudes. As shown in Figure 2a, there is a slight difference in r_{eff} as a function of CN concentration under very clean conditions (optical depth ≈ 0.2), but not of the magnitude reported by Kaufman and Fraser. Thus our results do not support their hypothesis.

2) The data used by Kaufman and Fraser may be affected by stratus clouds. Their average number-weighted cloud area was $\sim 5 \text{ km}^2$, but the area-weighted cloud area was $\sim 500 \text{ km}^2$. This implies that the data were influenced by large clouds. Clouds with areas of $\sim 500 \text{ km}^2$ and large vertical development, which would likely have ice near their tops, were excluded from the data analyzed by Kaufman and Fraser. Hence it is likely that their data were influenced, in part, by stratiform clouds. The data from section 5.2 of the present paper show that stratiform clouds have larger r_{eff} values than cumulus clouds with the same LWC and that the r_{eff} of stratiform clouds may be more susceptible to changes in smoke particle concentrations than cumulus clouds. Thus Kaufman and Fraser may have observed the susceptibility of stratocumulus clouds to changes in updraft velocity and CCN concentration.

3) Kaufman and Fraser's retrieval may have been influenced by cloud shape. Figure 8 shows a typical cumulus field in smoky haze over Porto Velho, Brazil. From this photograph one can see the difficulty in retrieving cloud properties from 1 km resolution satellite measurements. Because of high temperatures in the tropics, clouds can have significant vertical development and still remain warm. In inverting AVHRR data, Kaufman and Fraser assumed that the

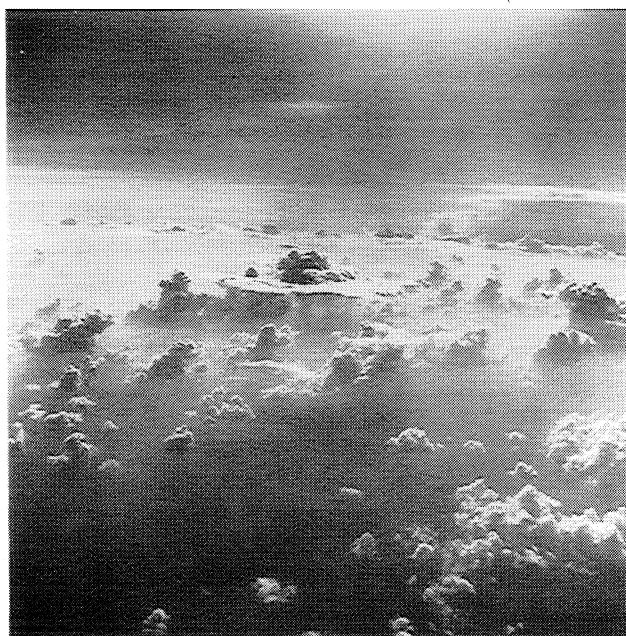


Figure 8. Cumulus clouds embedded in a haze dominated by smoke from biomass burning near Porto Velho, Brazil.

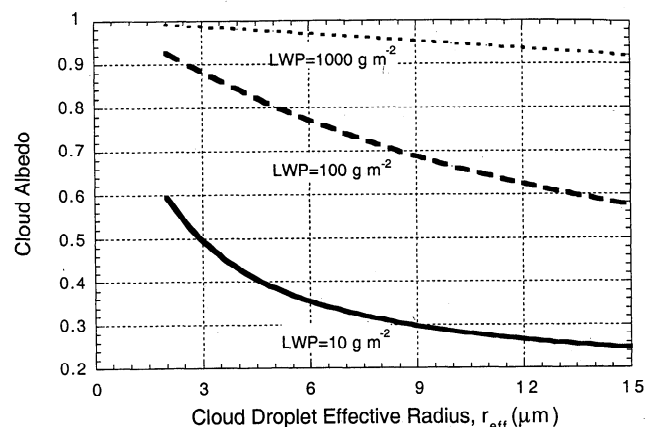


Figure 9. Model results for cloud albedo versus cloud droplet effective radius for three liquid water paths (LWP).

clouds were "plane parallel" in form with a $\pm 10^\circ$ slope. However, as seen in Figure 8, clouds in Brazil exhibit larger slopes. It is unclear how such vertical development affects cloud retrievals.

4) It is possible that the data presented in the present paper are weighted toward the lower and middle portions of clouds, while Kaufman and Fraser's r_{eff} values apply near cloud tops.

The difference between the results of Kaufman and Fraser [1997] and the data presented in the present paper adds to the uncertainty of indirect radiative forcing by smoke aerosols. It is certainly advantageous to measure cloud reflectivities (and hence indirect radiative forcing) directly as Kaufman and Fraser have done. However, many cloud models use r_{eff} to parameterize cloud reflectivity. In Figure 9, cloud albedo is plotted as a function of r_{eff} from a discrete ordinate radiative transfer model [Stamnes *et al.*, 1988] for a Sun zenith angle of 0° , a wavelength of 550 nm, and a surface albedo of 0.15. Results are plotted for three liquid water paths (LWP): 10 g m^{-2} to simulate thin clouds (e.g., cumulus humilis, altocumulus, and stratocumulus), 100 g m^{-2} to simulate clouds with moderate vertical development (e.g., cumulus mediocris), and 1000 g m^{-2} to simulate clouds with strong vertical development (e.g., cumulus congestus). Figure 9 shows that for clouds with albedos greater than about 0.35 and LWP of 10 to 100 g m^{-2} (such as those measured by Kaufman and Fraser), the cloud albedo is sensitive to r_{eff} . Kaufman and Fraser studied warm clouds, with low vertical development, and derived values for r_{eff} of $\sim 10 \mu\text{m}$. In this paper we have derived r_{eff} values of $\sim 7 \mu\text{m}$. Assuming a LWP of 10 g m^{-2} , we see from Figure 9 that these values of r_{eff} yield cloud albedos of 0.28 and 0.35 for Kaufman and Fraser's and our r_{eff} value, respectively. Hence the uncertainty of the effect of smoke particles on clouds is high.

8. Conclusions

The main conclusions of this study can be summarized as follows.

1) For accumulation-mode particle concentrations greater than $\sim 3000\text{--}4000 \text{ cm}^{-3}$, perturbations in smoke particle concentrations (up to $150,000 \text{ cm}^{-3}$) do not have a significant effect on the effective droplet radius (r_{eff}) of cumulus clouds in Brazil. Therefore for these cases, r_{eff} can be fairly well

estimated if the LWC is known. While the simple power law parameterization proposed by Martin *et al.* [1994] and Bower *et al.* [1994] for continental cumulus cloud adequately describes the r_{eff} versus LWC relationship for these clouds, the regression coefficient can be improved significantly if an arccosh function is used (see equation (6)).

2) It appears that stratocumulus clouds are more susceptible to ambient particle concentrations than cumulus clouds (Figure 3). Therefore r_{eff} for these clouds is not easily parameterized in terms of LWC alone.

3) The best parameterization for r_{eff} is as a function of LWC/N, rather than LWC alone (Figures 4 and 5).

4) Cloud droplet effective radii for clouds in Brazil affected by biomass smoke are much smaller than for clouds in cleaner marine environments. However, the r_{eff} versus LWC and r_{eff} versus LWC/N relationships for the cumulus clouds in Brazil that we studied are similar to those for cumulus clouds off the Atlantic seaboard of the United States. Hence in cumulus cloud models, smoke particles from biomass burning can be treated like any other anthropogenic pollutant, albeit smoke particles are often present in much higher concentrations.

5) For clouds in Brazil embedded in smoke hazes, we found r_{eff} values 2-5 μm lower than those derived by Kaufman and Fraser [1997] from satellite measurements. This leads to significant uncertainties in quantifying the effects of biomass burning on indirect radiative forcing.

Acknowledgments. The authors are grateful to Ashwin Mahesh, University of Washington, for producing the model results shown in Figure 8. This research was supported by the following grants: NASA NGT-30335, NGT5-30094, NAGW-3750, and NAG 1-1709; NSF ATM-9408941 and ATM-9400760; NOAA NA37RJ0198AM09 and NA67RJ0155 (JISAO contribution number 582); and EPA CR822077-01-0.

References

- Artaxo, P., F. Gerab, M. A. Yamasoe, and J. V. Martins, Fine mode aerosol composition at three long-term atmospheric monitoring sites in the Amazon Basin, *J. Geophys. Res.*, **99**, 22,857-22,868, 1994.
- Baumgardner, D., An analysis and comparison of five water droplet measuring instruments, *J. Appl. Meteorol.*, **22**, 891-910, 1983.
- Baumgardner, D., W. A. Cooper, and J. E. Dye, Optical and electronic limitations of the forward scattering spectrometer probe, in *Liquid Particle Size Measurement Techniques*, vol. 2, Rep. ATMS STP 1083, edited by E. D. Hirtleman, W. D. Bachalo, and P. G. Felton, pp. 115-127, Am. Soc. for Test. and Mater., Philadelphia, Pa., 1990.
- Blyth, A. M., and J. Latham, A climatological parameterization for cumulus clouds, *J. Atmos. Sci.*, **48**, 2367-2371, 1991.
- Bower, K. N., T. W. Choularton, J. Latham, J. Nelson, M. Baker, and J. Jensen, A parameterization of warm clouds for use in atmospheric general circulation models, *J. Atmos. Sci.*, **51**, 2722-2732, 1994.
- Garrett, T. J., and P. V. Hobbs, Long-range transport of continental aerosols over the Atlantic Ocean and their effects on cloud structures, *J. Atmos. Sci.*, **52**, 2977-2984, 1995.
- Gerber, H., Microphysics of marine stratocumulus clouds with two drizzle modes, *J. Atmos. Sci.*, **53**, 1649-1662, 1996.
- Gerber, H., B. G. Arends, and A. S. Ackerman, New microphysics sensor for aircraft use, *Atmos. Res.*, **31**, 235-252, 1994.

- Hansen, J. E., and L. D. Travis, Light scattering in planetary atmospheres, *Space Sci. Rev.*, **14**, 527-610, 1974.
- Hobbs, P. V., and L. F. Radke, Cloud condensation nuclei from a simulated forest fire, *Science*, **163**, 279-280, 1969.
- Hobbs, P. V., J. S. Reid, R. A. Kotchenruther, R. J. Ferek, and R. Weiss, Direct radiative forcing by smoke from biomass burning, *Science*, **275**, 1776-1778, 1997.
- Kaufman, Y. J., and R. S. Fraser, The effect of smoke particles on clouds and climate forcing, *Science*, **277**, 1636-1639, 1997.
- Kaufman, Y. J., and T. Nakajima, Effect of Amazon smoke on cloud microphysics and albedo, *J. Appl. Meteorol.*, **32**, 729-744, 1993.
- Kaufman, Y. J., A. Setzer, D. Ward, D. Tanre, B. N. Holben, P. Menzel, M. C. Pereira, and R. Rasmussen, Biomass Burning Airborne and Spaceborne Experiment in the Amazonas (BASE-A), *J. Geophys. Res.*, **97**, 14,581-14,599, 1992.
- Kaufman, Y. J., et al., The Smoke, Clouds, and Radiation-Brazil (SCAR-B) experiment, *J. Geophys. Res.*, **103**, 31,783-31,080, 1998.
- Kotchenruther, R. A., and P. V. Hobbs, Humidification factors of aerosols from biomass burning in Brazil, *J. Geophys. Res.*, **103**, 32,081-32,089, 1998.
- Leitch, W. R., G. A. Isaac, J. W. Strapp, C. M. Banic, and H. A. Weibe, The relationship between cloud droplet number concentrations and anthropogenic pollution: Observations and climatic implications, *J. Geophys. Res.*, **97**, 2463-2474, 1992.
- Liu, Y., and J. Hallett, The "1/3" power law between effective radius and liquid-water content, *Q. J. R. Meteorol. Soc.*, **123**, 1789-1795, 1997.
- Martin, G. M., D. W. Johnson, and A. Spice, The measurement and parameterization of effective radius of droplets in warm stratocumulus clouds, *J. Atmos. Sci.*, **51**, 1823-1842, 1994.
- Novakov, T., C. Rivera-Carpio, J. E. Penner, and C. F. Rogers, The effect of anthropogenic sulfate aerosols on marine cloud droplet concentrations, *Tellus*, **46B**, 132-141, 1994.
- Reid, J. S., P. V. Hobbs, R. J. Ferek, D. R. Blake, J. V. Martins, M. R. Dunlap, and C. Liousse, Physical, chemical, and optical properties of regional hazes dominated by smoke in Brazil, *J. Geophys. Res.*, **103**, 32,059-32,080, 1998.
- Ross, J., P. V. Hobbs, and B. Holben, Radiative characteristics of regional hazes dominated by smoke from biomass burning in Brazil: Closure tests and direct radiative forcing, *J. Geophys. Res.*, **103**, 31,925-31,941, 1998.
- Russell, P. B., P. V. Hobbs, and L. L. Stowe, Aerosol properties and radiative effects in the U.S. east coast haze plume: An overview of the Tropospheric Aerosol Radiative Forcing Observational Experiment (TARFOX), *J. Geophys. Res.*, in press, 1999.
- Stamnes, K., S. C. Tsay, W. Wiscombe, and K. Jayaweera, A numerically stable algorithm for discrete ordinate method radiative transfer in multiple scattering and emitting layered media, *Appl. Opt.*, **27**, 2502-2509, 1988.
- Twomey, S., The nuclei of natural cloud formation, II, The supersaturation in natural clouds and the variation of cloud droplet concentration, *Geophys. Pura Appl.*, **43**, 243-249, 1959.
- Warner, J., and S. Twomey, The production of cloud nuclei by cane fires and the effect on cloud droplet concentration, *J. Atmos. Sci.*, **4**, 704-706, 1967.

D. A. Hegg, P. V. Hobbs, and A. L. Rangno. Department of Atmospheric Sciences, University of Washington, Box 351640, Seattle, WA 98195-1640. (e-mail: deanhegg@atmos.washington.edu; phobbs@atmos.washington.edu; art@atmos.washington.edu)

J. S. Reid, Propagation Division, Space and Naval Warfare System Center, San Diego, CA 92152-7385. (e-mail: jreid@nosc.mil)

(Received July 21, 1998; revised December 10, 1998; accepted December 16, 1998.)